Available online at www.sciencedirect.com
ScienceDirect
Catalysis Today 137 (2008) 335–339
CATALYSIS TODAY
www.elsevier.com/locate/cattod

Nanostructured macro-mesoporous zirconia impregnated by noble metal for catalytic total oxidation of toluene

H.L. Tidahy [a], M. Hosseni [a], S. Siffert [a,*], R. Cousin [a], J.-F. Lamonier [a,c], A. Aboukaïs [a], B.-L. Su [b], J.-M. Giraudon [c], G. Leclercq [c]

[a] *Laboratoire de Catalyse et Environnement, E.A. 2598, Université du Littoral Côte d'Opale, 145 avenue Schumann, 59140 Dunkerque, France*
[b] *Laboratoire de Chimie des Matériaux Inorganiques, Facultés universitaires Notre Dame de la Paix, 61 rue de Bruxelles, 5000 Namur, Belgium*
[c] *Unité de Catalyse et Chimie du Solide, Université des Sciences et Technologies de Lille, Bât C3, 59655 Villeneuve d'Ascq, France*

Available online 28 November 2007

Abstract

Hierarchical bimodal macro-mesoporous zirconia oxide has been synthesized by a simple method in the presence of CTMABr surfactant. The synthesized zirconia having uniform macropores of 300–600 nm in diameter with wormhole-like mesoporous walls and high surface area was calcined at 400 and 600 °C and impregnated with 0.5 wt.% of palladium and compared with classical 0.5 wt.% Pd/ZrO_2 catalyst for toluene oxidation. The highest activity of 0.5 wt.%/macro-mesoporous zirconia calcined at 600 °C was mainly explained by a rather high Pd dispersion and by H_2-TPR measurements showing a higher quantity of PdO species easily reducible at 0 °C.

Keywords: Macro-mesoporous zirconia; Palladium; Toluene oxidation

1. Introduction

Volatile organic compounds (VOCs) emitted from industrial processes and automobile exhaust emissions represent a serious environmental problem, because of their toxic properties and their involvement in the formation of photochemical smog. Assessing the available technology for the removal of VOCs from polluted air stream, catalytic oxidation is one of the most promising [1]. Several catalysts are widely investigated for the total oxidation of VOCs [2–9], though deactivation of catalysts in the oxidation of VOCs is a challenge [10,11]. Among them, noble-metal-based (e.g. Pt and Pd) catalysts show the highest activity and selectivity for the oxidation of VOCs [2–4]. However, it is found that the support nature plays an important role in improvement of the efficiency of the catalyst, particularly in oxidation reaction. ZrO_2 is a very interesting material since lability and easiness to exchange oxygen atoms of the tetragonal phase make zirconia suitable for redox catalysis [7,12] as oxidations [13,14]. Indeed, Pd/ZrO_2 was found to be a high potential catalyst for toluene oxidation [15]. Moreover recently many nanostructured mesoporous oxides with high surface area and uniform pore size distribution are used as support for multiple catalyst applications [16–18]. For example, nanostructured porous zirconia, titania, and binary zirconium and titanium oxides for palladium catalysts have provided excellent catalytic properties for complete toluene and chlorobenzene oxidation [18]. This previous studies have shown that catalytic activities of supported palladium are greatly affected by the nature of the support. The observed high catalytic activity of Pd/mesoporous titania in complete oxidation of these VOCs could be connected with the reducibility of PdO particles and adsorption enthalpy of toluene.

The main goal of the current work is to improve the high activity of Pd/ZrO_2 catalyst for VOCs oxidation. Therefore, we examine the influence of the pre-treatment of a new porous zirconia on the total oxidation of toluene over the palladium supported catalysts. We have thus synthesized hierarchical bimodal macro-mesoporous zirconium oxide by a simple method in the presence of a single surfactant [18–21]. The synthesized zirconia particles are amorphous, having uniform macropores of 300–600 nm in diameter with wormhole-like mesoporous walls and high surface area.

* Corresponding author. Tel.: +33 3 28 65 82 56.
E-mail address: siffert@univ-littoral.fr (S. Siffert).

0920-5861/$ – see front matter © 2007 Elsevier B.V. All rights reserved.
doi:10.1016/j.cattod.2007.09.008

2. Experimental

2.1. Zirconia support preparation

The macro-mesoporous zirconia is prepared by the method described in Ref. [21]. 15 wt.% micellar solution of cetyltrimethylammonium bromide (CTMABr) is prepared by dissolving CTMABr in an aqueous acidic solution (pH 2) at 40 °C under stirring for at least 3 h. An appropriated content of zirconium propoxide ($Zr(OC_3H_7)_4$) is added dropwise into the above solution with a surfactant/Zr molar ratio of 0.33. After further stirring for 1 h, the mixture is transferred into a Teflon-lined autoclave, and heated at 60 °C for 2 days. The product is filtered by Soxhlet extraction with ethanol for at least 30 h in order to remove the surfactant species. The final sample is dried at 60 °C at called mesoZrO_2. Then a part of sample as prepared are calcined in air at 400 °C (mesoZrO_2-400) and at 600 °C (mesoZrO_2-600) for 4 h.

2.2. Catalysts preparation

Pd supported by zirconia catalysts are prepared by aqueous impregnating method using palladium nitrate ($Pd(NO_3)_2{\cdot}XH_2O$, Johnson Matthey). The impregnated powders are dried at 100 °C overnight and calcined in air at 400 °C for 4 h.

Pd/mesoZrO_2, Pd/mesoZrO_2-400 and Pd/mesoZrO_2-600 are prepared by impregnating with 0.5 wt.% Pd content on porous supports.

For comparison, a reference zirconia sample is prepared by precipitation of a precursor salt solution by ammonium according to the procedure described in Ref. [7]. After its calcination in air at 600 °C, palladium supported on a classical zirconia, called Pd/ZrO_2-ref, is also prepared by the same procedure as described above.

2.3. Characterization techniques

The structures of solids are analysed by powder X-ray diffraction (XRD) technique at room temperature with a Bruker diffractometer using Cu Kα radiation scanning 2θ angles ranging from 10° to 80°.

The nitrogen adsorption analysis is performed on Sorptomatic 1990 apparatus at −196 °C and the specific surface areas of the solids are determined by BET method.

The temperature programmed reduction (TPR) experiments are carried out in an Altamira AMI-200 apparatus. The TPR profiles are obtained by passing a 5% H_2/Ar flow (30 mL min^{-1}) through the calcined sample (about 100 mg). The temperature is increased from −40 to 300 °C at a rate of 5 °C min^{-1}. The hydrogen concentration in the effluent is continuously monitored by a thermoconductivity detector (TCD).

Pulse chemisorption measurements are performed using the same apparatus. The samples are pre-treated for 2 h in a flow of hydrogen at 200 °C, in order to reduce the Pd in the catalyst. The samples are then cooled to 100 °C in a stream of argon. Pulse chemisorption measurements are performed at this temperature with 5% H_2/Ar.

Toluene oxidation is carried out in a conventional fixed bed microreactor and studied between 25 and 300 °C (1 °C min^{-1}). The reactive flow (100 N mL min^{-1}) is composed of air and 1000 ppm of gaseous toluene. The analysis of combustion products is performed evaluating the toluene conversion and the $CO/(CO + CO_2)$ molar ratio from a Perkin Elmer autosystem chromatograph equipped with TCD and FID. Before the catalytic test, the solid (100 mg) is calcined under a flow of air (2 L h^{-1}) at 400 °C (1 °C min^{-1}) and reduced under hydrogen flow (2 L h^{-1}) at 200 °C.

3. Results and discussion

3.1. Physico-chemical characterization

Scanning electron microscopy (SEM) and transmission electron microscopy (TEM) of synthesized macro-mesoporous zirconia material presenting in Ref. [18] shown that the zirconia macro-mesoporous particles used as catalyst support in this work have a size of around 10 μm (SEM image) [20,21]. The synthesized zirconia particles contain regular arrays of macropores having a diameter range from 300 to 500 nm. The hollow macrochannels are always orthogonal to the face of the monolithic particle (TEM image). Moreover, macroporous walls are mesostructured with a disordered wormhole-like assembly of meso-micropores into macroporous framework.

X-ray diffraction patterns of porous zirconia are shown in Fig. 1A. Untreated mesoZrO_2 zirconia framework possesses a global amorphous structure (Fig. 1A.a). After calcination at 400 °C, the crystallization of amorphous zirconia to a tetragonal phase is observed, intense line appeared at $2\theta = 30.2°$ (Fig. 1A.b). When the solid is calcined at 600 °C the intensity of preceding line increase and other line appears at 28.2°, this latter indicates that a monoclinic phase of zirconia is formed (Fig. 1A.c). The XRD pattern of the classical zirconia shown in Fig. 1A.d presents only the tetragonal phase of zirconia.

Fig. 1B shows XRD patterns of palladium-based catalyst. The addition of palladium on mesoZrO_2-400 and mesoZrO_2-600 does not structurally perturb the nature of the already pre-treated support (Fig. 1B.b and c). But for Pd/mesoZrO_2 catalyst (Fig. 1B.a), tetragonal character of zirconia is obtained due to the calcination of the solid after palladium impregnation. Nevertheless, in comparison with Fig. 1A.b, i.e. the 400 °C-calcined sample of mesoZrO_2, the intensity of the latter is lower than the former; the presence of Pd could delay the crystallization of ZrO_2. As Pd loading is rather low with 0.5% Pd/zirconia samples, the absence of diffraction lines of PdO is due to the high dispersion degree of the supported phase and/or the low palladium content. The XRD pattern of the Pd/ZrO_2-ref (not shown) is like the spectra of classical zirconia shown in Fig. 1A.d.

The textural properties in terms of BET surface area, pore volume and average pore size of solids are summarized in Table 1.

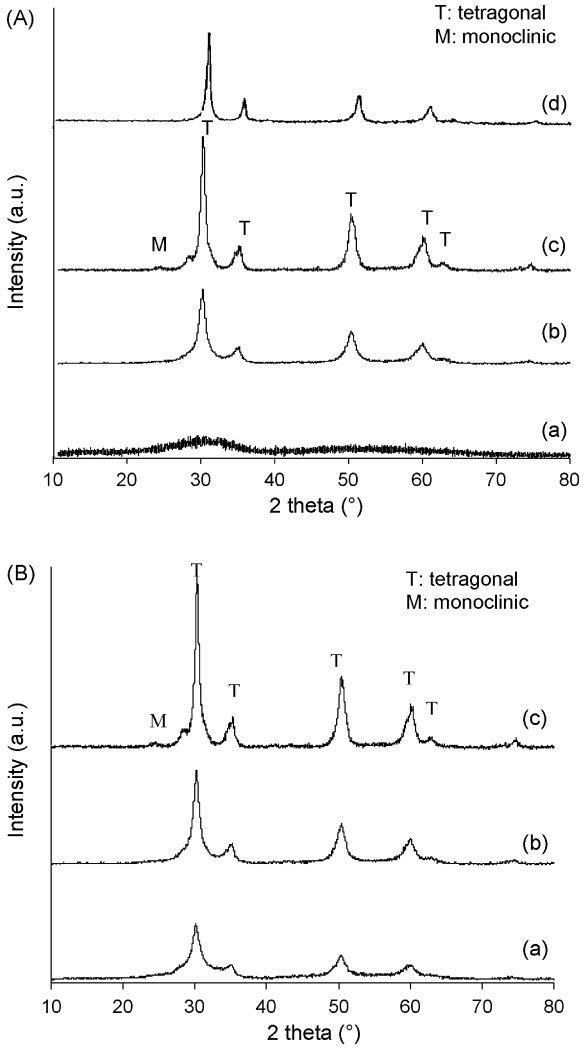

Fig. 1. (A) XRD patterns of porous materials: (a) mesoZrO$_2$ (untreated sample), (b) mesoZrO$_2$-400 (sample calcined at 400 °C), (c) mesoZrO$_2$-600 (sample calcined at 600 °C) and (d) XRD pattern of the classical ZrO$_2$-ref sample. (B) XRD patterns of calcined palladium-based catalysts: (a) Pd/mesoZrO$_2$, (b) Pd/mesoZrO$_2$-400 and (c) Pd/mesoZrO$_2$-600.

The surface area and porous volume of the pure mesoporous zirconia is sharply decreased after the calcination at 400 and 600 °C. The crystallization of the walls separating mesopores leading to partial destruction of the porous structure should explain this decrease (XRD data). It is interesting to observe that the pore diameter for mesoZrO$_2$-600 is larger than that of mesoZrO$_2$-400. Pd incorporation leads to a decrease of the surface areas for Pd/mesoZrO$_2$-400 and Pd/mesoZrO$_2$-600, but the average pore diameters are unchanged.

In the case of the Pd/ZrO$_2$-ref, its characterization leads to the following properties, tetragonal and monoclinic phase like Pd/mesoZrO$_2$-600 and surface area 88 m^2 g^{-1} lower than the 100 m^2 g^{-1} of Pd/mesoZrO$_2$-600.

Pd dispersion and Pd particle size of the catalysts are presented in Table 1. Pd dispersion can be correlated to the specific surface for Pd/mesoZrO$_2$-400, Pd/mesoZrO$_2$-600 and Pd/ZrO$_2$-ref. The Pd particles size should be on the outer surface or into the macropores for the porous zirconia samples.

The reducibility of supported palladium oxide is an important factor influencing its catalytic property [22]. We actually observed on palladium-based catalysts [23,24] that the reduction step before the catalytic test allowed protecting the catalyst from coke deposit and obtaining a stable active catalyst with metallic Pd particles. The H$_2$-TPR profiles of calcined catalysts are displayed in Fig. 2A. Apparently, observed changes of the TPR profiles indicate variations in the distribution of palladium oxide with support type and its calcinations. Moreover, in all cases the signals of H$_2$ consumption correspond to complete reduction of PdO to Pd^0 [25,26].

For the Pd/mesoZrO$_2$-600 and 0.5% Pd/ZrO$_2$-ref (Fig. 2A.c and d), PdO is easily reducible, and the H$_2$-consumption peaks are observed at lower temperature at about 0 °C followed by a negative H$_2$-consumption peak observed at 80 °C which can be attributed to the desorption of hydrogen adsorbed on the metallic palladium [27,28] forming palladium hydrides. These results indicate that both supports could have quite similar structure and Pd particles have a similar distribution. However, the sample 0.5% Pd/mesoZrO$_2$-600 seems to have a higher H$_2$-consumption peak. This could be due to the existence of some metallic Pd species on 0.5% Pd/ZrO$_2$-ref before TPR experiment.

For Pd/mesoZrO$_2$ and Pd/mesoZrO$_2$-400 catalyst (Fig. 2A.a and b), PdO reduction occurred in two times for Pd/mesoZrO$_2$ and three times for Pd/mesoZrO$_2$-400. It can be assumed to a non-uniform distribution of Pd particles with a first one at near −22 °C attributed to the reduction of smaller PdO particles on the surface (easily reducible), a second peak appearing at 11 °C assigned to the reduction of bulky particles for Pd/mesoZrO$_2$-400

Table 1
Main physico-chemical properties of zirconia supports and catalysts

Sample	S_{BET} (m^2 g^{-1})	Pore size (nm)	Pore volume (cm^3 g^{-1})	Palladium dispersion[a] (%)	Palladium particle size[a] (nm)
MesoZrO$_2$	463	1.2	0.364	–	–
MesoZrO$_2$-400	184	1.2	0.223	–	–
MesoZrO$_2$-600	102	1.8	0.142	–	–
Pd/mesoZrO$_2$	222	1.2	0.357	54	2.1
Pd/mesoZrO$_2$-400	150	1.2	0.211	64	1.7
Pd/mesoZrO$_2$-600	100	1.8	0.141	40	2.8
Pd/ZrO$_2$-ref	88	–	–	30	3.7

[a] Determined from H$_2$ chemisorption at 100 °C.

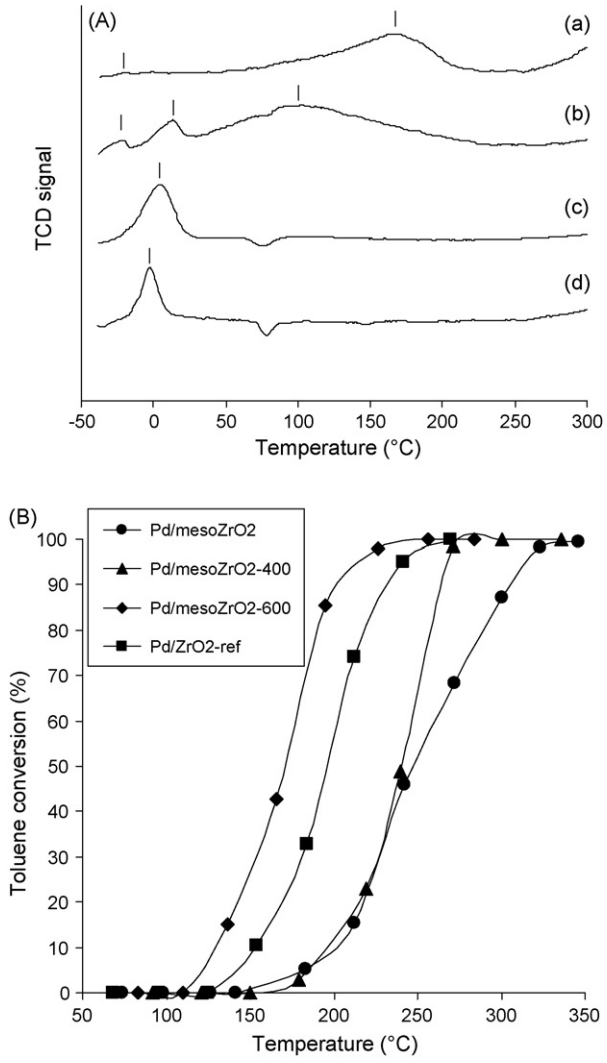

Fig. 2. (A) TPR profiles of 0.5% Pd/zirconia catalysts: (a) Pd/mesoZrO$_2$, (b) Pd/mesoZrO$_2$-400, (c) Pd/mesoZrO$_2$-600 and (d) Pd/ZrO$_2$-ref. (B) Toluene conversion versus temperature for 0.5% Pd/zirconia catalysts.

and the last centred at 102 °C for Pd/mesoZrO$_2$-400 and at 165 °C for Pd/mesoZrO$_2$ related to the reduction of PdO species probably in the pores and partially protected from the reduction by a ZrO$_2$ coverage. Thus a partial degradation of the porous structure after palladium impregnation should occur (loss of specific area and crystallization) and could lead to this ZrO$_2$ coverage of palladium. Moreover, the reducibility of the Pd oxides depends on their dimensions as the decomposition of the corresponding Pd hydrides. In fact the lower the Pd dispersion the higher is the reducibility of the corresponding PdO particles (Fig. 2A) and the intensity of the negative peak corresponding to Pd hydrides.

3.2. Catalytic performance in the total oxidation of toluene

In Fig. 2B, catalytic activity data of catalysts are compared. The observed products are only carbon dioxide and water, indicating complete oxidation occurring during reaction. The general order of catalysts activity for toluene oxidation is Pd/mesoZrO$_2$-600 > Pd/ZrO$_2$-ref > Pd/mesoZrO$_2$-400 > Pd/mesoZrO$_2$.

The Pd/mesoZrO$_2$-600 exhibits the highest catalytic activity in comparison with the other samples. This result is surprising since the specific area of Pd/mesoZrO$_2$ and Pd/mesoZrO$_2$-400 and their Pd dispersion are higher than that of Pd/mesoZrO$_2$-600 (Table 1). The reason of this catalytic behaviour can be related to the much easier reducibility of palladium species for Pd/mesoZrO$_2$-600. Pd/ZrO$_2$-ref and Pd/mesoZrO$_2$-600 exhibit similar structure of zirconia support and close TPR profiles. Therefore the higher Pd dispersion for Pd/mesoZrO$_2$-600 than Pd/ZrO$_2$-ref can explain the difference of activity.

If we compare the activity order for toluene oxidation and the TPR profiles, it seems that the quantity of PdO species reducible at around 0 °C can also be correlated to the activity. In fact, the quantity of PdO species reducible at around 0 °C for palladium-based catalysts increases from Pd/mesoZrO$_2$ to Pd/mesoZrO$_2$-400 via Pd/ZrO$_2$-ref to Pd/mesoZrO$_2$-600. Those kinds of species easily reducible must be the more active Pd particles for toluene oxidation. Okumura et al. [29] have observed the influence of the pre-treatment of support on the electronic interaction between palladium particles and support. The acidic–basic properties of the support influence the Pd oxidation and that the co-existence of Pd and PdO species on the Pd surface is important for VOC oxidation [30]. Thus the mechanism of toluene oxidation should undergo by a first oxidation of PdO by O_2 to form very active [$Pd^{2+}O^{2-}$] species which oxidize the hydrocarbon and Pd^{2+} cation is reduced to Pd^0. The activity of Pd should be controlled be reducibility of PdO by the hydrocarbon and then through the electronic interaction between the support and palladium. The reduction step should then be an important factor for the catalytic activity. Consequently pre-treatment of support could decrease the electronic interaction between palladium particles and zirconia and then leads to easier reducible palladium particles and a more active catalyst.

4. Conclusion

High performing classical Pd/ZrO$_2$ catalyst for VOCs oxidation can be improved by the use of macro-mesoporous zirconia support calcined at 600 °C instead of classical high surface area commercial zirconia. The highest activity of 0.5 wt.%/macro-mesoporous zirconia calcined at 600 °C was meanly explained by a better Pd dispersion and by TPR measurements showing a higher quantity of PdO species easily reducible. Indeed the mechanism of toluene oxidation should undergo a first oxidation of PdO by O_2 to form very active [$Pd^{2+}O^{2-}$] species which oxidize the hydrocarbon and Pd^{2+} cation is reduced to Pd^0.

Acknowledgments

The authors thank the European community through an Interreg IIIa France-Wallonie-Flandre project and Walloon Region for financial supports.

References

[1] T. Garcia, B. Solosona, D. Cazorla-Amoros, A. Linares-Solano, S.H. Taylor, Appl. Catal. B 62 (2006) 66–76.
[2] J.J. Spivey, Ind. Eng. Chem. Res. 26 (1987) 2165–2180.
[3] T. Maillet, C. Solleau, J. Barbier, D. Duprez, Appl. Catal. B 14 (1997) 85–95.
[4] J. Carpentier, J.-F. Lamonier, S. Siffert, E.A. Zhilinskaya, A. Aboukaïs, Appl. Catal. A 234 (2002) 91–101.
[5] M. Ferrandon, E. Björnbom, J. Catal. 200 (2001) 148–159.
[6] Y. Liu, M. Luo, Z. Wei, Q. Xin, P. Ying, C. Li, Appl. Catal. B 29 (2001) 61–67.
[7] M. Labaki, S. Siffert, J.-F. Lamonier, E.A. Zhilinskaya, A. Aboukaïs, Appl. Catal. B 43 (2003) 261–271.
[8] W.B. Li, W.B. Chu, M. Zhuang, J. Hua, Catal. Today 93–95 (2004) 205–209.
[9] H.G. Lintz, K. Wittstock, Catal. Today 29 (1996) 457–461.
[10] J.J. Spivey, J.B. Butt, Catal. Today 11 (1992) 465–500.
[11] S.K. Ihm, Y.D. Jun, D.C. Kim, K.E. Jeong, Catal. Today 93–95 (2004) 149–154.
[12] A. Martinez-Arras, M. Fernandez-Garcia, C. Belver, J.C. Conesa, J. Soria, Catal. Lett. 65 (2000) 197.
[13] D. Terribile, A. Trovarelli, C. de Leitenburg, A. Primavera, G. Dolcetti, Catal. Today 47 (1999) 133–140.
[14] J.-F. Lamonier, N. Sergent, J. Matta, A. Aboukais, J. Therm. Anal. Calorim. 66 (2001) 645–658.
[15] H.L. Tidahy, S. Siffert, F. Wyrwalski, J.-F. Lamonier, A. Aboukaïs, Catal. Today 119 (2007) 317.
[16] V. Idakiev, L. Ilieva, D. Andreeva, J.-L. Blin, L. Gigot, B.-L. Su, Appl. Catal. A 243 (2003) 25–29.
[17] V. Idakiev, T. Tabakova, Z.Y. Yuan, B.-L. Su, Appl. Catal. A 270 (2004) 135–141.
[18] H.L. Tidahy, S. Siffert, J.-F. Lamonier, E.A. Zhilinskaya, A. Aboukaïs, Z.-Y. Yuan, A. Vantomme, B.-L. Su, X. Canet, G. De Weireld, M. Frère, T.B. N'Guyen, J.-M. Giraudon, G. Leclercq, Appl. Catal. A 310 (2007) 61–69.
[19] Z.Y. Yuan, T.Z. Ren, A. Vantomme, B.-L. Su, Chem. Mater. 16 (2004) 5096–5106.
[20] J.-L. Blin, A. Léonard, Z.Y. Yuan, L. Gigot, A. Vantomme, A.K. Cheetham, B.-L. Su, Angew. Chem. Int. Ed. 42 (2003) 2875–12875.
[21] Z.Y. Yuan, A. Vantomme, A. Léonard, B.-L. Su, Chem. Commun. (2003) 1558–1559.
[22] W. Lin, Y.X. Zhu, N.Z. Wu, Y.C. Xie, I. Murwani, E. Kemnitz, Appl. Catal. B 50 (2004) 59–66.
[23] J. Jacquemin, S. Siffert, J.-F. Lamonier, E.A. Zhilinskaya, A. Aboukais, Stud. Surf. Sci. Catal. 142 (2002) 699–706.
[24] H.L. Tidahy, Thesis of the University of Littoral, Dunkerque, France, 2006.
[25] S.T. Homeyer, W.M.H. Sachtler, J. Catal. 117 (1989) 91–101.
[26] W.J. Shen, M. Okumura, Y. Matsumura, M. Haruta, Appl. Catal. A 213 (2001) 225–232.
[27] M.L. Cubeiro, J.L.G. Fierro, Appl. Catal. A 168 (1998) 307–322.
[28] G. Neri, M.G. Musolino, C. Milone, D. Pietropaolo, S. Galvagno, Appl. Catal. A 208 (2001) 307–316.
[29] K. Okumura, T. Kobayashi, H. Tanaka, M. Niwa, Appl. Catal. B 44 (2003) 325–331.
[30] P. Dégé, Thesis of the University of Poitiers, France, 1999.